Modeling of Two-Phase Flows

Kurt O. Lund*
Engineering Consultant to SML Associates
* 135 Sixth Street, Del Mar, CA 92014; kurtlund@roadrunner.com

Abstract: Viscous equations are developed for regions with two interacting flowing fluids, or two fluid phases, such as occur in fluidized particle beds or the mixing of fluids. The descriptive equations are rendered into the standard COMSOL PDE matrix form, and solved over typical two-dimensional regions, as time-dependent interacting laminar flows. The model geometry selected is that of a, so called, spouted fluidized bed in which a two-dimensional jet of gas is injected into a bed of particles. The resulting interface shear stress between the gas and the particles is modeled with a typical shear parameter, and viscous effects are included in the viscous terms with effective viscosities. The results show the effect of the developing jet, the particle circulation, and the distribution of the void fraction.

Keywords: CFD, two-phase, laminar flow, fluidized bed.

1. Introduction

Regions with two interacting flowing fluids, or fluid phases, occur in many important applications, ranging from fluidized particle beds to the mixing of fluids. Such regions are notoriously difficult to model because the intermingling of one phase with the other introduces effective compressibility into the otherwise incompressible descriptive differential equations; few CFD software packages have capability for more than a single phase.

Traditionally, model equations have been mostly inviscid with various empirical terms accounting for compressibility and inter-fluid shear, such as the pioneering work of Gidaspow and his students[1, 2]; these were usually solved with finite difference approximations over simple regions, and sometimes by method of characteristics as for hyperbolic equations and compressible flow. More recent formulations include general viscosity, and even turbulence models[3, 4] The inclusion of (constant) viscosity renders the equations elliptical in space as the NS equations; however, problems with bounded sensitivities can cause integration difficulties.

A particular advantage of the COMSOL software is that it is not restricted to packaged model equations nor simple geometries, but allows the direct input of "custom" model equations for finite element approximations over complex regions. Here, two-dimensional, interacting viscous equations for two-phase fluids are derived in transport format, and rendered into the general PDE form that allows direct input to the COMSOL Finite Element software.

The model geometry selected is that of a, so called, spouted fluidized bed in which a two-dimensional jet with particles is injected into a volume. This causes shear stress between the gas and the particles, thus driving the particles in a circulation cell, a behavior that can be important for various chemical and thermal processes. The results show the effect of the developing jet, the particle circulation, and the distribution of the void fraction.

2. Problem Formulation

The viscous equations for two-phase flows are very close to the standard Navier-Stokes equations, except for the void and solid fractions that affect the working densities, and for the inter-phase shear. Usually, these mass and momentum relations are stated in conservation form[1-4]; however, for COMSOL implementation, it is convenient to state them in the usual transport form, as shown in **Appendix A** for constant gas- and solid-phase densities, ρ_g and ρ_s. These are 6 equations to solve for u_g, v_g, u_s, v_s, p, and ε, with $\sigma = 1 - \varepsilon$.

The momentum equations (2) and (3) will be recognized as close to the usual NS equations, but with effective densities, $\varepsilon\rho_g$ and $\sigma\rho_s$, where ε is the void fraction and $\sigma = 1 - \varepsilon$ is the solid fraction (these fractions appear in the mass equations (1) and cause compressibility effects).

The viscous terms in (2) and (3) frequently include normal stress effects[3,4]; however, to simplify and demonstrate feasibility of approach, viscosity is limited here to the usual shear-

effects, with gas- and solid-phase viscosities, η_g and η_s.

The inter-phase friction coefficient, β [kg/s.m^3], is usually based on the Ergun equation[1-4], which is an empirical correlation of drag effects on the particles, and a strong function of void fraction; typical values are shown in Fig. 1:

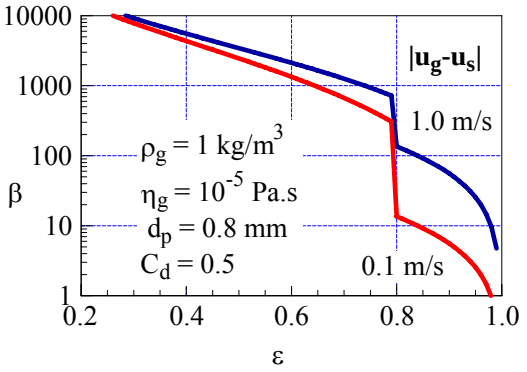

Figure 1. Inter-phase friction parameter β [kg/s.m^3] as a function of void fraction.

For the purpose of demonstrating computational feasibility, β is here treated as a known parameter.

Usually, all second-order terms require two boundary conditions in elliptical equations; however, the presence of the algebraic β-terms has an important effect on boundary conditions: If both u_g and u_s are specified, for example, then the β-terms introduce an algebraic constraint that may be extraneous and difficult to meet; therefore, where u_g is specified at an inlet boundary, u_s will be left unspecified.

The COMSOL general PDE form is given by

$$d_a(\partial\vec{u}/\partial t) + \vec{\nabla} \bullet \Gamma = \vec{F}$$

where the d_a's are coefficients (e.g., densities), Γ is a matrix of the terms with the highest derivatives (i.e., the viscous terms), and F is a vector of forcing functions (here including convective terms). To facilitate input to this form, the descriptive equations are written in matrix form in **Appendix B**, where the comma denotes partial differentiation.

3. Computational Results

The test problem under consideration is an 80 cm wide by 2 m high (long) trough with a 20 cm inlet slot at the bottom (left), shown on its side in Fig. 2a with laminar NS flow:

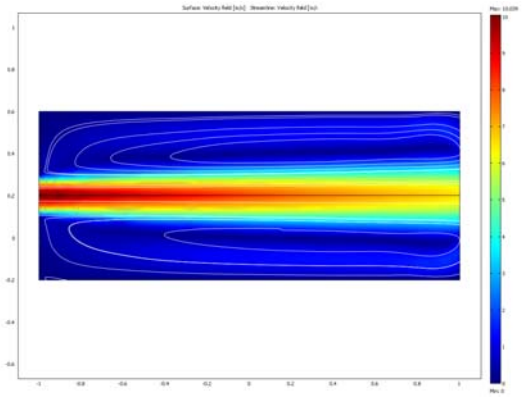

Figure 2a. Test-problem geometry with single-fluid steady-state Navier-Stokes flow(max/min = 10/0 m/s).

3.1 Qualification

As a prelude to two-phase flow, and to qualify the programming, the steady-state flow distribution for a single-phase gas was determined, as shown in Fig. 2a, using the COMSOL Navier-Stokes solver. The gas properties are ρ_g = 1 kg/m^3, η_g = 1 cPa.s, and the jet inlet is specified parabolic laminar flow with a center-line velocity of 10 m/s, which corresponds to an inlet Reynolds number of 400.

In a time-dependent calculation, starting with the trough gas at rest, the flow field in Fig. 2b was reached in 350 ms.

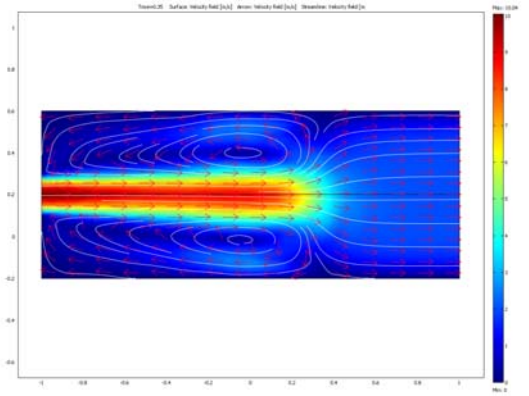

Figure 2b. Test-problem geometry with single-fluid time-dep. Navier-Stokes flow (max/min = 10/0 m/s).

If the above problem is simulated by setting the inter-phase shear to a small number (β = 0.001 kg/s.m^3), and integrating the two-phase equations in **Appendix B**, then at t = 350 ms the pattern in Fig. 3 is reached.

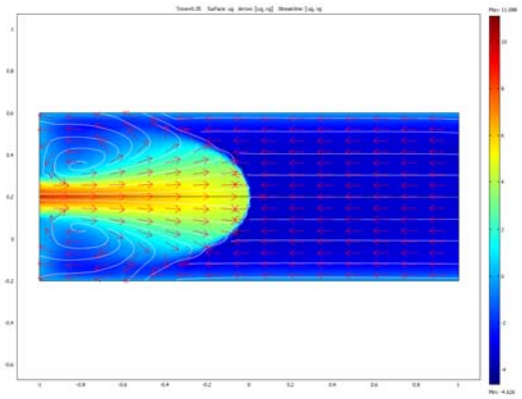

Figure 3. Test-problem geometry with two-fluid time-dependent flow and small inter-phase shear (max/min ≈ 10/-4 m/s).

It is seen that the penetration is similar to the NS solution at 350 ms, but that there is a shock-like sharp boundary beyond which a negative axial flow develops; at this front the arrows show that the stream directions meet and feed into the circulation by the jet boundary. During the flow development, the sharp front was seen to proceed from the left entrance (gravitational bottom) in a steady fashion. This flow field is a consequence of the varying void fraction, and its effect on the mass equations; it is not possible in the NS flow in Fig. 2 where the gas flow exits the right (top of the trough) because it would violate conservation of mass. In both calculations, Neuman conditions (or zero slope) were specified for the velocities at the "outlet", and the pressure and void fraction were specified.

3.2 Two-Phase Results

In experiments with spouted beds, it has been found difficult to start up with a packed bed, and then forming the desired gas jet into it; instead, startup begins with gas flow into the volume and gradual addition of solid phase[5]. This approach is modeled here with the inlet solid fraction increasing from 0 to 35% over 300 ms, as shown in Fig. 4. The inlet gas velocity is parabolic laminar flow with a peak velocity of 10 m/s; the solids velocity is unspecified, but determined from the shear parameter, set at $\beta = 10$ kg/s.m^3. The (computational) gas is *very* viscous with $\eta_g = 1$ cPa.s (10 centipoise); $\rho_g = 1$ kg/m^3, which yields an inlet Reynolds number of 400; the solid phase is taken as 20 times this density, and 100 times the viscosity ($\rho_s = 20$ kg/m^3, $\eta_s = 1$ Pa.s). It is noted that these are model fluids for the computation; the high viscosity facilitated convergence of the time steps.

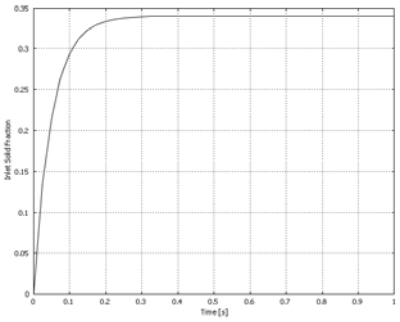

Figure 4. Inlet Solid Fraction.

The axial gas and solids velocity fields for these conditions, and at t = 1 s, are shown in Figs. 5a and 5b, along with corresponding streamlines and direction arrows.

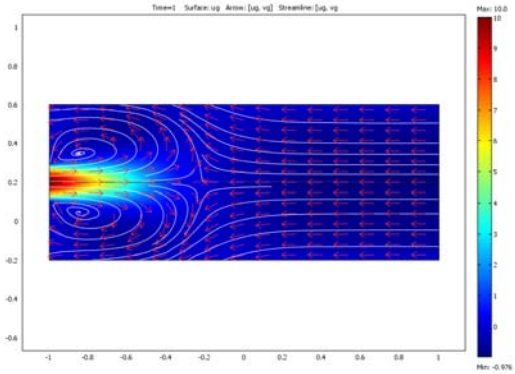

Figure 5a. Gas axial velocity at t = 1 s, for $u_{g,in} = 10$ m/s and $\beta = 10$ kg/s.m^3 (max/min ≈ 10/-1 m/s).

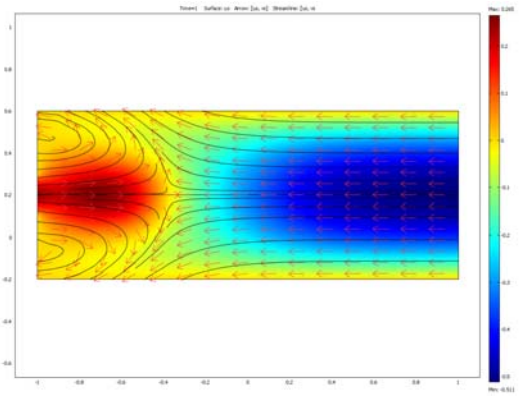

Figure 5b. Solids axial velocity at t = 1 s, for $u_{g,in}$ = 10 m/s and β = 10 kg/s.m^3(max/min ≈ 0.2/-0.5 m/s).

It is seen in Fig. 5a that the inlet jet penetrates only a short distance, surrounded by gas recirculation inside the flow-front. This penetration proceeded smoothly from the inlet to the present location in about 350 ms; thus, at t = 1 s, these distributions are close to a steady state.

In Fig. 5b, the positive solids velocity, u_s (dragged along by u_g) has a maximum of about 0.2 m/s, but a larger negative value (where u_g is small) due to gravity and higher density. Although flow appears to exit the side walls, these have specified zero slip and normal velocities, and u_g, v_g, u_s, and v_s are all zero here.

The flow-reversal front corresponds to a relatively rapid change in pressure, as shown in Fig. 5c; as seen, the pressure is near constant behind the front (red color), but is reduced in front of it (yellow to blue) until zero at the top.

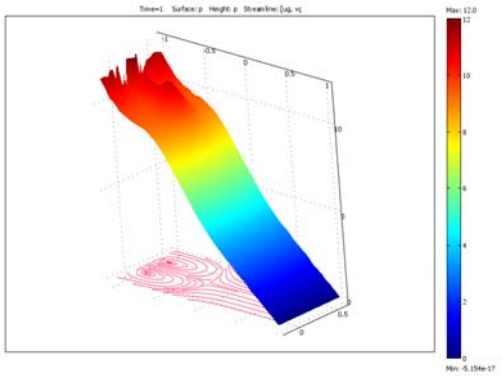

Figure 5c. Pressure field at t = 1 s, for $u_{g,in}$ = 10 m/s and β = 10 kg/s.m^3.

The corresponding solid fraction is shown in Fig. 5d, the inlet peak being 35%; it shows a similar penetration as the gas velocity in Fig. 5a.

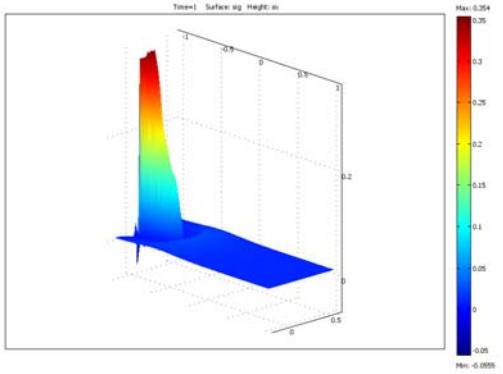

Figure 5d. Solid fraction, σ, at t = 1 s, for $u_{g,in}$ = 10 m/s and β = 10 kg/s.m^3 (max/min ≈ 0.35/0).

The flow in a horizontal jet (with gravity "turned off") is show in Fig. 6, where the flow proceeds uniformly from inlet to outlet.

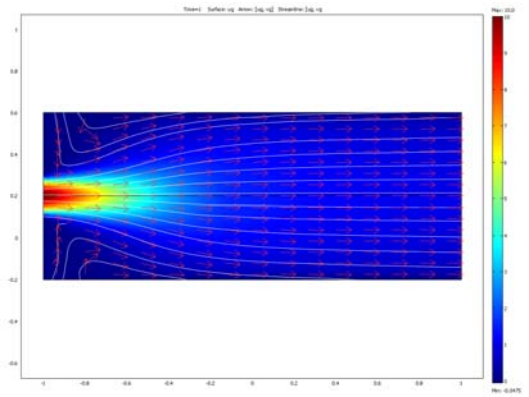

Figure 6. Gas *horizontal* velocity at t = 1 s, for $u_{g,in}$ = 10 m/s and β = 10 kg/s.m^3 (max/min ≈ 10/0 m/s).

As a final calculation, the inlet velocity was changed to 25 m/s, or Re_{in} = 1,000. The result for a *vertical* trough is shown in Figs. 7a and 7b.

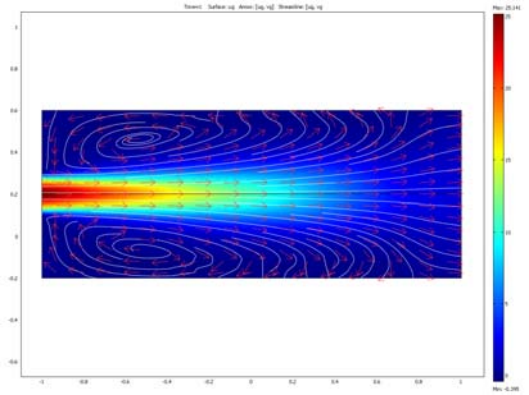

Figure 7a. Gas axial velocity at t = 1 s, for $u_{g,in}$ = 25 m/s and β = 10 kg/s.m^3 (max/min ≈ 25/0 m/s).

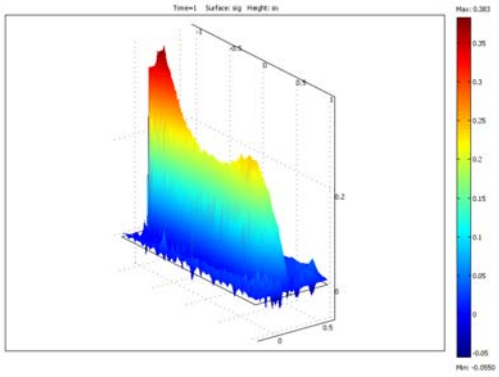

Figure 7b. Solid fraction, σ, at t = 1 s, for $u_{g,in}$ = 25 m/s and β = 10 kg/s.m^3 (max/min ≈ 0.35/0).

Here it is seen that some solid phase extends nearly to the outlet, and that the flow proceeds positively to the exit due to the higher jet momentum. However, when the shear was changed to β = 100 kg/s.m^3 shorter jet penetration and flow reversal occurred, with a distribution similar to Fig. 5a. A calculation with β determined from Fig. 1 became unstable after only a few milliseconds.

4. Discussion

The present results demonstrate the solution of two-phase transport equations using the COMSOL PDE modeling and the built-in Finite Element solvers. These transport equations appear similar to the single-phase NS equations, and therefore would appear to be solvable by the same techniques; however, inclusion of the void fraction as a variable introduces added degrees of freedom that can cause compressibility effects, as shown in Figs. 5.

In particular, the results are sensitive to the coupling parameter, β, in relation to the inlet jet boundary condition. Many integration attempts included inlet conditions on both the solid- and the gas-phase; however, the problem then appeared to be over-constrained by the algebraic coupling parameter, β. Better convergence was achieved by eliminating the solid-phase condition.

Inlet gas flows larger than 25 m/s (Re_{in} > 1,000) were also attempted, but without convergence. Laminar flows become physically (and numerically) unstable at these Reynolds numbers; applications with higher jet velocities will likely require a turbulence model in the gas phase, including law-of-the-wall variables.

Larger values of β tended to further attenuate the inlet jet penetration. In the present model problem, the largest velocity difference is at the inlet, causing a very large β-value there when the correlation in Fig. 1 was used; in this case there was practically no flow development with the instantaneous initial inlet gas velocity specified.

Inclusion of viscosity in the model equations renders the equations elliptical in space (and parabolic in time), which is well suited to the finite element solution techniques. However, normal gas viscosities are too small to achieve convergence of the time steps (at least for $u_{g,in}$ = 10 m/s), and therefore were increased for the computational gas. Another problem presents itself as the very large solid-phase density (usually > 1,000 kg/m^3), in comparison to that of the gas. The gravitational forces on this phase are very large, and exceedingly small time increments would be required to obtain solutions.

5. Conclusions

This paper has examined the use of the COMSOL finite element modeling technique for laminar two-phase flows, as applied to a spouted fluidized-bed type geometry. By placing the transport equations in the PDE matrix form, direct input to the software was achieved, and solutions obtained with built-in solvers.

Further two-phase modeling should evaluate normal stress effects in the solid phase, and turbulence modeling in the gas phase, as well as extending the analysis to three dimensions.

6. References

1. Gidaspow, D, Hydrodynamics of Fluidization and Heat Transfer: Supercomputer Modeling, *Applied Mechanics Review*, **Volume 39**, No. 1, pp 1-22 (1986)

2. Gidaspow, D, *Multiphase Flow and Fluidization*, page numbers. Academic Press, New York (1994)

3. Ibsen, C. H. et al., A Study of Dilute to Dense Flow in a Circulating Fluidized Bed, *Int'l. Symp. Multiphase Flow and Transport Phenomena (MFTP-2000)*, Antalya, Turkey, 5-10 November (2000)

4. Ibsen, C. H. et al., Evaluation of a Three-Dimensional Numerical Model of a Scaled Circulating Fluidized Bed, *IECR, United Eng. Foundation-CRE VIII*, Barga, Italy, 23-29 June (2001)

5. Lord, S. M., Personal Communication, SML Associates, 109 Peppertree Lane, Encinitas, CA 92024 (2007).

7. Acknowledgements

The author wishes to acknowledge the encouragement of Stephen Lord for this project, and the partial support of SML Associates,
www.smlassociates.com

Appendix A: Transport Equations

Conservation of Mass

Gas: $$\frac{\partial \varepsilon}{\partial t}+\frac{\partial}{\partial x}\left(\varepsilon u_g\right)+\frac{\partial}{\partial y}\left(\varepsilon v_g\right)=0=\frac{\partial \varepsilon}{\partial t}+\varepsilon\left(\frac{\partial u_g}{\partial x}+\frac{\partial v_g}{\partial y}\right)+u_g\frac{\partial \varepsilon}{\partial x}+v_g\frac{\partial \varepsilon}{\partial y} \quad \textbf{(1a)}$$

Solid: $$\frac{\partial \sigma}{\partial t}+\frac{\partial}{\partial x}\left(\sigma u_s\right)+\frac{\partial}{\partial y}\left(\sigma v_s\right)=0=-\frac{\partial \varepsilon}{\partial t}+\sigma\left(\frac{\partial u_s}{\partial x}+\frac{\partial v_s}{\partial y}\right)-u_s\frac{\partial \varepsilon}{\partial x}-v_s\frac{\partial \varepsilon}{\partial y} \quad \textbf{(1b)}$$

Gas-Phase Momentum Equations

$$\rho_g\varepsilon\left\{\frac{\partial u_g}{\partial t}+u_g\frac{\partial u_g}{\partial x}+v_g\frac{\partial u_g}{\partial y}\right\}=-\varepsilon\frac{\partial p}{\partial x}+\beta(u_s-u_g)+\rho_g\varepsilon g_{gx}+\eta_g\left(\frac{\partial^2 u_g}{\partial x^2}+\frac{\partial^2 u_g}{\partial y^2}\right) \quad \textbf{(2a)}$$

$$\rho_g\varepsilon\left\{\frac{\partial v_g}{\partial t}+u_g\frac{\partial v_g}{\partial x}+v_g\frac{\partial v_g}{\partial y}\right\}=-\varepsilon\frac{\partial p}{\partial y}+\beta(v_s-v_g)+\rho_g\varepsilon g_{gy}+\eta_g\left(\frac{\partial^2 v_g}{\partial x^2}+\frac{\partial^2 v_g}{\partial y^2}\right) \quad \textbf{(2b)}$$

Solid-Phase Momentum Equations

$$\rho_s\sigma\left\{\frac{\partial u_s}{\partial t}+u_s\frac{\partial u_s}{\partial x}+v_s\frac{\partial u_s}{\partial y}\right\}=-\sigma\frac{\partial p}{\partial x}+\beta(u_g-u_s)+\rho_s\sigma g_{sx}+\eta_s\left(\frac{\partial^2 u_s}{\partial x^2}+\frac{\partial^2 u_s}{\partial y^2}\right) \quad \textbf{(3a)}$$

$$\rho_s\sigma\left\{\frac{\partial v_s}{\partial t}+u_s\frac{\partial v_s}{\partial x}+v_s\frac{\partial v_s}{\partial y}\right\}=-\sigma\frac{\partial p}{\partial y}+\beta(v_g-v_s)+\rho_s\sigma g_{sy}+\eta_s\left(\frac{\partial^2 v_s}{\partial x^2}+\frac{\partial^2 v_s}{\partial y^2}\right) \quad \textbf{(3b)}$$

Appendix B: COMSOL Input PDF Equations

$$\frac{\partial}{\partial t}\begin{Bmatrix}-\varepsilon\\+\varepsilon\end{Bmatrix}=\begin{Bmatrix}\varepsilon\left(u_{g,x}+v_{g,y}\right)+u_g\varepsilon_{,x}+v_g\varepsilon_{,y}\\ \sigma\left(u_{s,x}+v_{s,y}\right)-u_s\varepsilon_{,x}-v_s\varepsilon_{,y}\end{Bmatrix}$$

$$\rho_g\varepsilon\frac{\partial}{\partial t}\begin{Bmatrix}u_g\\v_g\end{Bmatrix}+\begin{bmatrix}-\eta_g u_{g,x} & -\eta_g u_{g,y}\\ -\eta_g v_{g,x} & -\eta_g v_{g,y}\end{bmatrix}\begin{Bmatrix}\frac{\partial}{\partial x}\\ \frac{\partial}{\partial y}\end{Bmatrix}=\begin{Bmatrix}-\varepsilon p_{,x}+\beta(u_s-u_g)-\rho_g\varepsilon\left(u_g u_{g,x}+v_g u_{g,y}-g_{gx}\right)\\ -\varepsilon p_{,y}+\beta(v_s-v_g)-\rho_g\varepsilon\left(u_g v_{g,x}+v_g v_{g,y}-g_{gy}\right)\end{Bmatrix}$$

$$\rho_s\sigma\frac{\partial}{\partial t}\begin{Bmatrix}u_s\\v_s\end{Bmatrix}+\begin{bmatrix}-\eta_s u_{s,x} & -\eta_s u_{s,y}\\ -\eta_s v_{s,x} & -\eta_s v_{s,y}\end{bmatrix}\begin{Bmatrix}\frac{\partial}{\partial x}\\ \frac{\partial}{\partial y}\end{Bmatrix}=\begin{Bmatrix}-\sigma p_{,x}+\beta(u_g-u_s)-\rho_s\sigma\left(u_s u_{s,x}+v_s u_{s,y}-g_{sx}\right)\\ -\sigma p_{,y}+\beta(v_g-v_s)-\rho_s\sigma\left(u_s v_{s,x}+v_s v_{s,y}-g_{sy}\right)\end{Bmatrix}$$